Available online at www.sciencedirect.com
SCIENCE DIRECT®
Journal of Sound and Vibration 284 (2005) 1015–1031
JOURNAL OF SOUND AND VIBRATION
www.elsevier.com/locate/jsvi

Assessment of fresco detachments through a non-invasive acoustic method

Dionisio Del Vescovo*, Annalisa Fregolent

Dipartimento di Meccanica e Aeronautica, Università di Roma "La Sapienza", Via Eudossiana 18, 00184 Roma, Italy

Received 14 July 2003; received in revised form 6 May 2004; accepted 26 July 2004
Available online 15 December 2004

Abstract

In artistic frescoes, the partial detachment of plaster portions is a typical and serious problem. At present, the standard procedure of diagnosis consists of manual inspection, but produces only approximate information. This work describes in more detail an acoustic, non-invasive, experimental technique of diagnosis, which has been already proposed by the authors. It is based on the acoustic–structural interaction which occurs when an acoustic duct is excited by a loudspeaker and closed by the investigated fresco at the opposite end. The analysis of the acoustic pressure field and of its alterations allows the assessment of detachments, since the acoustic modal parameters are affected by the acoustic system boundary conditions, i.e. the portion of fresco closing the duct. Experiments carried out on fresco specimens show the potential of this acoustic method.

1. Introduction

An important part of the artistic heritage throughout the world is represented by historical buildings, whose finish layer often consists of plaster. Among these, frescoes are precious works of art deserving considerable efforts for proper conservation. Fresco is an artistic wall-painting technique consisting of the application of water-colours on a fresh plaster layer. The plaster is

*Corresponding author. Tel.: +39 06 44 58 52 09; fax: +39 06 48 48 54.
E-mail addresses: dionisio.delvescovo@uniroma1.it (D. Del Vescovo), annalisa.fregolent@uniroma1.it (A. Fregolent).

0022-460X/$ - see front matter © 2004 Elsevier Ltd. All rights reserved.
doi:10.1016/j.jsv.2004.07.011

made of lime paste, sand and marble sawdust and is generally composed of three different layers: the deepest, formed by a coarse mortar, called *arriccio*; a smoother, intermediate layer on which the artist would sketch a preliminary drawing with a sharp tip; and a thin plaster finish made of a finer mortar, named *intonachino*, which was painted in fresco.

Fresco degradation can be caused by several external agents involving physical, chemical and/or biological factors, like structure displacements, vibrations, temperature changes, humidity, pollution and mildew. A typical initial defect is local delamination between plaster layers or between plaster and the substratum. Progressively, air and humidity, which are trapped in the cavities created by this loss of cohesion, can cause the painted layer to crack and flake away. To avoid further damage an early detection of the detached areas is crucial, inasmuch as it allows a timely fresco restoration.

At present, the traditional empirical method of diagnosis is still used. The restorer gently hits the fresco surface with his knuckles and, sensing the vibrations with his fingertips and listening to the different sounds, can detect the presence of detachments. This manual technique requires special skills in order to judge the impact force to be applied to the painted plaster, and to find out possible defects. Moreover, it provides no better results than a qualitative survey, it is time consuming and generally involves the use of scaffolding to reach the painted surface.

Recently, several methods based on automatic, non-invasive and faster procedures were proposed to avoid those disadvantages. These methods were borrowed from the research field on non-destructive testing (NDT) and adapted to the particular features of frescoes.

Thermal imaging [1–3] takes advantage of the variations of the thermal characteristics due to the air cavities generated by the detachments. Indeed, in spite of an initial homogeneous fresco heating, the different cooling speed relative to intact and detached areas causes a non-uniform temperature distribution. The diagnosis of the fresco conservation is obtained by monitoring the infrared radiation of the surface. This method is automatic and non-invasive, but expensive and time consuming.

The ultrasound technique [3–5] is based on the different sound velocity of media and on the consequent transmission time increase caused by discontinuities which generate air pockets and interfaces. Thus detachments can be detected measuring the time taken by an ultrasonic pulse between a transmitter and a receiver set in front of the fresco surface. This method is helpfully employed in metallic work of art inspection, but requires refinements for wall paintings.

Other methods rely on the structural dynamic behaviour [6]. Bonarrigo [7] analyses the dynamic response of mosaics to acoustic excitation. D'Ambrogio [8], in preliminary research, analyses the vibrations which are obtained exciting the structure with a low-level impact force and measuring the surface response with accelerometers; the frequency response functions (FRFs) of intact and detached areas show clear differences that imply a correlation between the detachments and the FRF shape. Castellini [9] determines the FRFs measuring the response with a scanning laser Doppler vibrometer which allows a fast examination of large areas of the fresco surface; this method is non-intrusive, does not necessarily imply the use of scaffolding, but requires an expensive apparatus. Calicchia [10] uses a Cepstral technique for evaluating the acoustic energy adsorption due to the structural modes acoustically excited; this method provides an acoustic image of the detachments and employs a non-invasive, inexpensive, portable apparatus.

This paper is an extended version of Ref. [11] in which a novel, acoustic, non-invasive technique is proposed. This technique is based on the analysis of the sound pressure field modifications

inside a rectilinear duct which interacts with the investigated fresco. Such modifications depend on the acoustic–structural interaction which is affected by the plaster preservation state. The research, which has been developed on some laboratory specimens accurately reproducing the structural fresco features, provides the guidelines for an effective method for the diagnosis of fresco detachments.

2. Methodology

The aim of the present method is to discover any detachment by analysing the vibration distribution of the frescoed plaster. Indeed, it had been observed that detachments show their presence through remarkable vibrations in limited areas [8–10]. Such vibrations are evaluated indirectly by dynamically coupling the structure with an appropriate acoustic device. It consists of a rectilinear acoustic duct, which is excited at one end by a loudspeaker and closed by the investigated fresco surface at the opposite end (Fig. 1). All the features of the acoustic system are known, except the boundary conditions resulting from the interaction with the fresco. Such boundary conditions depend on the dynamics of the closing structure, which in turn are affected by the plaster preservation state. In fact, when the closing wall is a portion of detached plaster, rather than a flawless one, a higher vibration level is excited by the acoustic waves. Consequently, the presence of detachments in the coupling area can be detected through the analysis of the acoustic field. The diagnosis procedure consists in scanning the frescoed plaster, coupling the acoustic device successively with different portions of the structure.

The following considerations are relevant to the experimental context described in Section 3.1, i.e. the three specimens in Fig. 8 and the two set-up arrangements defined in the first five rows of Table 1.

2.1. Functioning characteristics

The acoustic device can be modelled as an acoustic duct, sealed by a plane surface at one end and driven at the opposite end by a stiff, flat, oscillating piston. Moreover, as the duct diameter complies with the requirement of being sufficiently smaller than the wavelength in the frequency range of analysis, the piston generates plane waves perpendicular to the duct axis. Other design requirements are discussed in Section 3.1.

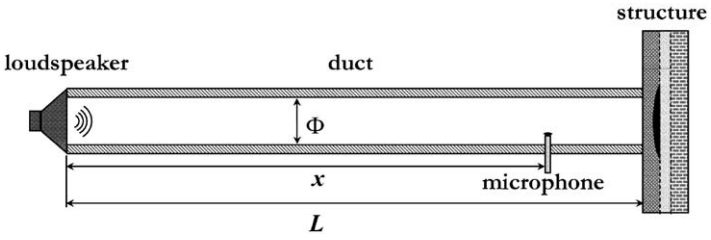

Fig. 1. Acoustic device.

Table 1
Acoustic device details

	Set-up 1	Set-up 2
Pipe diameter Φ	0.074 m	0.074 m
Pipe length L	0.511 m	0.323 m
Microphone–loudspeaker distance x	0.337 m	0.211 m
First/second resonance frequency	350/674 Hz	535/1061 Hz
First antiresonance frequency	497 Hz	768 Hz
Diagnosis frequency interval	400–620 Hz	620–920 Hz

Anticipating some results from later descriptions, the characteristics and functioning of the present method can be summed up as follows:

(a) By means of a loudspeaker, only the acoustic system is directly excited.
(b) The acoustic–structural interaction, limited to precise areas of both systems, causes a transfer of energy from the acoustic system to the structure; the surface of the structure, where it is coupled with the device, is loaded with plane waves with normal incidence.
(c) The acoustic–structural interaction depends on the features of the structure in the area where the two systems are coupled:
  (i) the flawless areas display nearly stiff behaviour towards the energy exchange;
  (ii) the detached areas allow an energy exchange, due to the compliance of the detachments; the exchange increases when the compliance increases.
(d) In presence of detachments in the coupling area, the acoustic–structural interaction produces effects in both the structure and the acoustic system.
  (i) In the structure it increases the local vibration level by means of a double mechanism: the global increment of the structure excitation due to the energy exchange augmentation and the local vibration increment due to the detachment compliance.
  (ii) In the acoustic system it causes the alteration of the sound pressure field. Two different phenomena are observed: the perturbation due to structural resonances and a net flow of the energy from the acoustic duct towards the structure.
(e) By means of microphones, the acoustic field is measured and analysed. Any perturbation can be related to the local level of the structural vibrations and to the exchange of energy between the acoustic system and the structure.

Because of the operational characteristics in items (a) and (e), this method is non-invasive and allows avoidance of expensive devices.

As mentioned in item (c), a portion of fresco without defects may be considered rigid and with this assumption the acoustic system response is completely known. Defining an acoustic FRF as the ratio between the sound pressure and the piston velocity, this hypothesis is confirmed in Figs. 2 and 3 where experimental FRFs pertaining to undamaged areas are compared with the corresponding analytic FRFs. The accordance is fairly good, except at low frequencies where the loudspeakers have a poor emission; furthermore, over about 1000 Hz the curves are indicative, because the acoustic duct does not comply with the hypothesis of plane waves anymore.

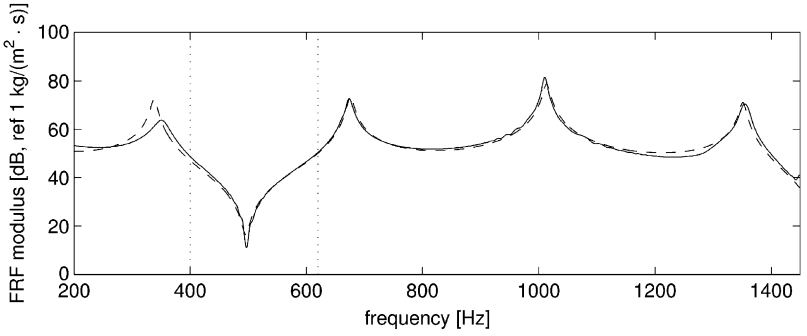

Fig. 2. Experimental (——) and analytic (– –) FRFs of the acoustic duct closed by a rigid wall for set-up 1.

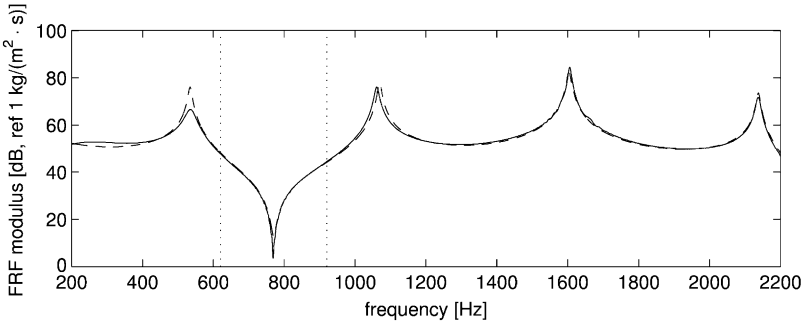

Fig. 3. Experimental (——) and analytic (– –) FRFs of the acoustic duct closed by a rigid wall for set-up 2.

The mentioned analytic FRFs are provided by the expression [12]

$$\Gamma(x,\omega) = \frac{p(x,\omega)}{u_0(\omega)} = \rho_0 c\,\frac{\cos[\omega\,(l-x)/c]}{\sin(\omega l/c)}, \tag{1}$$

where $\Gamma(x,\omega)$ is the acoustic FRF, x the pipe axial abscissa (see Fig. 1), ω the angular frequency, p the sound pressure, u_0 the piston velocity, ρ_0 the air density, l the pipe length and c the sound velocity in air. The dissipative effects are roughly taken into account considering c as a complex quantity. The resonances of the system are given by the roots of the denominator of Eq. (1):

$$f_n = \frac{nc}{2l}, \quad n = 0, 1, \ldots \tag{2}$$

and they depend on the length l of the duct. Letting the numerator of Eq. (1) equal to zero, the antiresonances of the system can be obtained as

$$z_m = \frac{2(m+1)}{4}\frac{c}{(l-x)}, \quad m = 0, 1, \ldots \tag{3}$$

and they depend on the microphone location x and the duct length l.

The situations reported in Figs. 2 and 3 are assumed as reference cases. Moreover, as later described, the acoustic–structural interaction is more evident around an acoustic antiresonance. For this reason, the diagnosis and the evaluation of the effects of the acoustic–structural interaction are performed in the frequency intervals between the pairs of vertical, dotted lines in Figs. 2 and 3.

2.2. Acoustic–structural interaction

For the double mechanism cited in item d(i), a detachment generates a raise of the local vibration level compared to the rigid hypothesis. Furthermore, both phenomena pointed out in item d(ii) are useful for the detachment assessment, because they cause distinctive modifications in the acoustic FRFs: (1) structural resonances evince their presence through some irregularities in both the modulus and the phase; (2) the net energy flow towards the structure produces an increment of the loss factor.

The two kinds of modifications of the acoustic FRF are illustrated through the following instances. The effect of structural resonances around an acoustic antiresonance is exhibited in Fig. 4, where an acoustic FRF relative to a detached area is shown together with the structural response, represented in a suitable fictitious scale: vibration peaks correspond to local minima of the acoustic response and vice versa. This is because the acoustic duct has a flexible vibrating closing wall as boundary condition. The effect of the energy flow is displayed in Fig. 5 where the FRFs of two different measures carried out in undamaged and detached plaster areas are compared: the increment of loss factor of the antiresonance is evident. This happens because the acoustic response is affected by the energy subtracted and dissipated on the part of the structure.

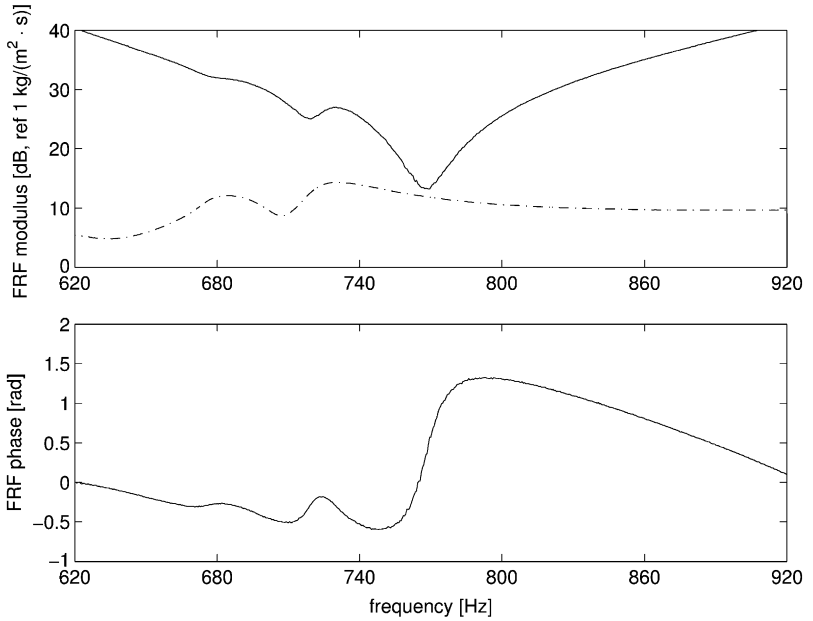

Fig. 4. Effects of structural response resonances (– · –) on acoustic FRF (——) for set-up 2 and Specimen 3.

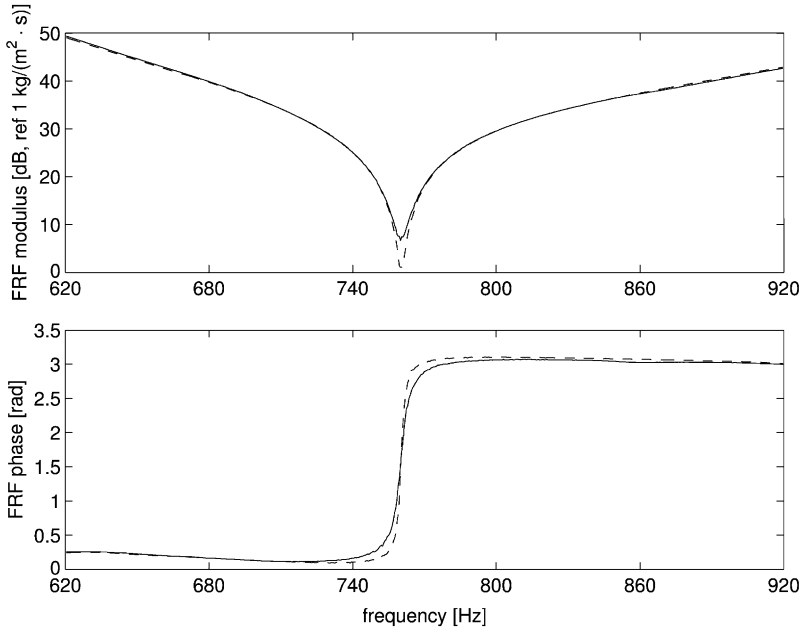

Fig. 5. Effects of energy exchange on acoustic FRF for set-up 2 and Specimen 2: detached area (——); undamaged area (– –).

2.3. Detachment indicator

It is possible to exploit both these distinctive acoustic FRFs modifications in order to define an indicator aimed at the detachment assessment. This is achieved by means of a proper model, which is formulated with two targets: *reproducing* the conformation around an antiresonance of the experimental acoustic FRF phase, evaluating the loss factor value and *not reproducing* the irregularities caused by the structural resonances. This model is represented by the following expression:

$$\Phi(\mu, \omega_n, a, b) = \tan^{-1}\left(\frac{2\mu\omega/\omega_n}{1-(\omega/\omega_n)^2}\right) + a(\mathrm{e}^{-b\omega} - 1). \tag{4}$$

The function $\Phi(\mu, \omega_n, a, b)$ is composed by an arctangent plus an empiric corrective term and depends on the loss factor μ, the natural frequency ω_n and the parameters a and b. The *detachment indicator* is evaluated by fitting the function Φ with the experimental data: in the case in which there are structural resonances, it takes into account the discrepancies between the experimental data and the model and this major contribution dominates the indicator value; in the opposite case it depends only on the raise of the loss factor μ and the corresponding contribution is less significant. So, although this latter effect is less evident, also when there are no structural resonances in the frequency interval of diagnosis, the detachment can be detected through the net energy flow. The indicator level is obtained weighting and combining appropriately the two

contributions. So, if the map of the indicator level is drawn throughout the inspected surface, then the detachments can be delineated.

In order to clarify how the indicator is estimated, few instances are reported. To estimate the net energy flow, the identified loss factor μ is monitored. To single out this situation, a case without perceivable structural resonances is shown in Fig. 6. It shows two pairs of curves: each pair represents the phase around an antiresonance of a measured acoustic FRF together with its best fit. One pair refers to the measure of a detached portion of fresco, whereas the other refers to a flawless one. In both situations the analytic and experimental curves are virtually overlaid. In the instance of the detached area, the loss factor is twice as much that of the flawless area: it is precisely such an increase to assess the presence of the detachment. Conversely, the effects of the structural resonances are taken into account through proper algorithms which quantify the discrepancies between the experimental phases and the fitted curves provided by Eq. (4). In Fig. 7, two typical instances are shown: in each figure the measure relative to a detached portion is reported together with its best fit. In both instances, the irregularities produced by the structural resonances are tangible and not matched by the model.

3. Experimental analysis

The observations reported in the previous section were developed with the aid of an experimental analysis, designed to highlight the effects of the interaction between the fresco and the acoustic waves inside the duct. Prior to commenting the obtained results, it is of some help for the comprehension to provide a few general considerations on some adopted solutions and the description of the laboratory set-up.

3.1. Experimental framework

The technique consists in using a loudspeaker to excite plane waves normal to the duct axis, and measuring with microphones, at definite locations along the axis, the acoustic field which results from the interaction with the portion of fresco which seals the duct. Since the cohesion state of the

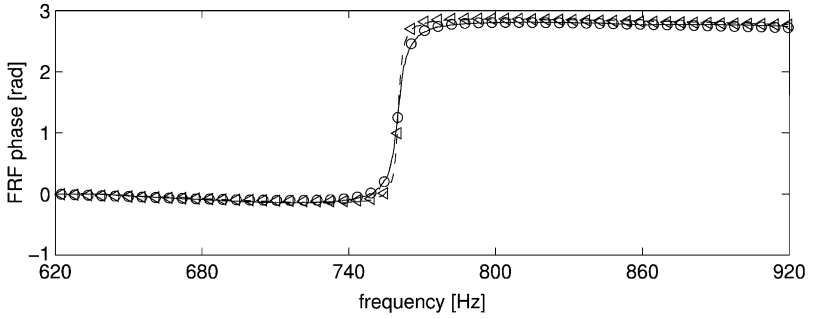

Fig. 6. Best fits in absence of structural resonances for set-up 2 and Specimen 2. Undamaged area: experimental phase (– –) and its best fit (◁) with $\mu = 0.0016$. Detached area: experimental phase (——) and its best fit (○) with $\mu = 0.0034$.

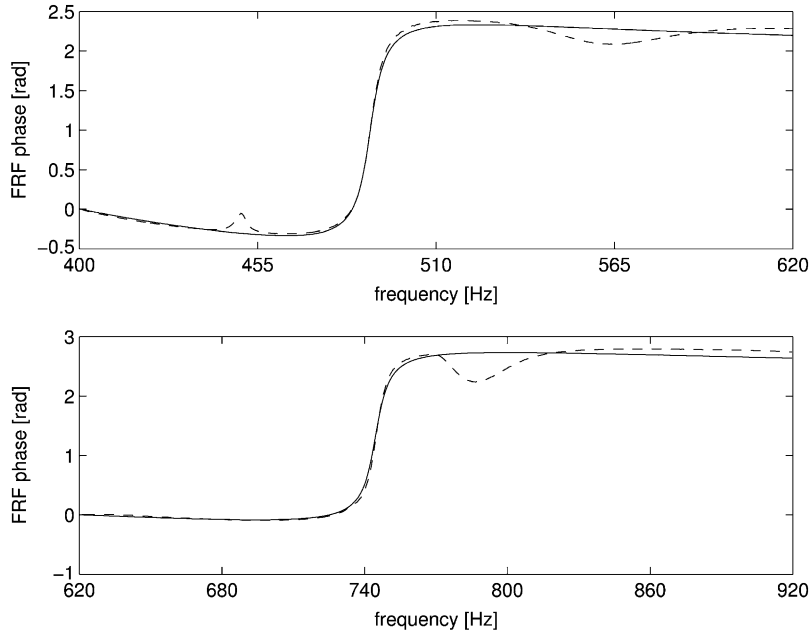

Fig. 7. Two typical instances of best fit with structural resonances respectively for set-up 1 and Specimen 3 (above) and for set-up 2 and Specimen 1 (below): experimental phase (– –) with its best fit (——).

fresco affects the acoustic field, by scanning in this way the whole wall surface to be inspected, the existence of detachments can be detected via comparative analysis of the results.

The specimens used for the experimental campaign were provided by the Opificio delle Pietre Dure in Florence (Italy), which is an Institute of the Ministry for Cultural Heritage, whose operational, research and training activities find expression in the field of conservation of works of art. The specimens are built in order to reproduce fresco structures and small detachments. They consist in an unglazed fired clay, simulating the underlying wall, on which two layers of plaster are spread. The two layers are made of lime mortar with varied particle-size sand. Indeed, the deeper layer is coarse-grained as in the *arriccio*, while the superficial one is fine-grained as in the *intonachino*. The detachments are generated with proper cavities which simulate the loss of cohesion. Apart from these common features, the lab specimens have heterogeneous characteristics in order to examine the various situations which occur in real frescoes. So different materials are employed and layers with various thickness are realized. Furthermore, the detachments were realized with different sizes and shapes and were located either between the two plastered layers or between the deeper plaster layer and the supporting clay. For obvious methodological reasons, size, shape and location of the detachments are known. An outstanding subset of three specimens (Fig. 8), having detachments with different size, depth and location, is utilised in this section for expositive purposes. These detachments represent a significant case study: in fact smaller ones are generally not considered for conservation treatments while larger ones are more compliant and therefore easier to locate. Although only few damage characteristics can be partially identified at the present stage in the development, the cited differences are still useful to appraise the technique sensitivity.

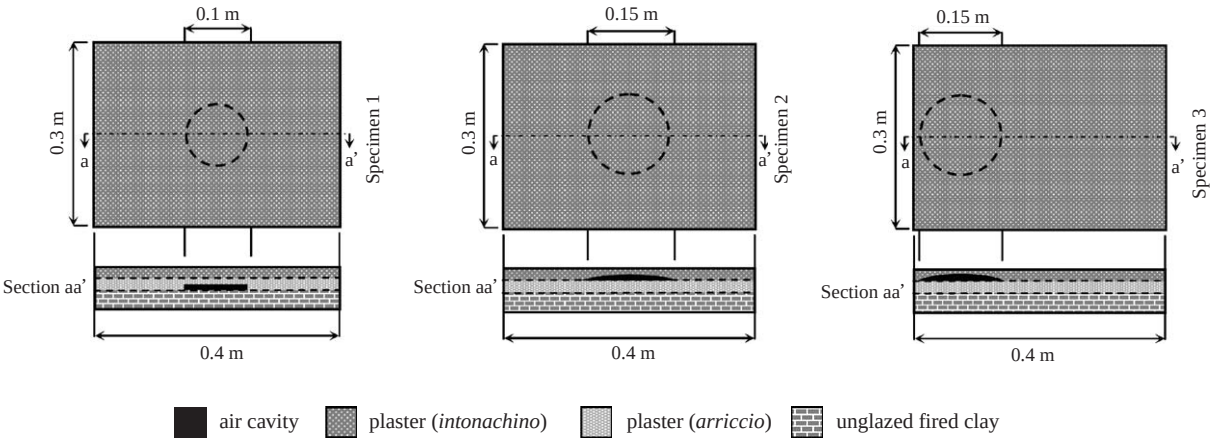

Fig. 8. Sketches of the fresco specimens.

Some elements should be taken into account to design an effective experimental set-up:

1. The vibration characteristics of the fresco structure and consequently the acoustic–structural interaction are strictly related to the frequency intervals of excitation.
2. It came out from the experimental analysis that the acoustic–structural interaction can be conveniently quantified in intervals around the acoustic antiresonances. This condition is further enhanced when these antiresonances are well separated from resonances, therefore when they are symmetrically sited between two resonances.
3. The pipe length L determines the natural frequencies and the gaps between them (Eq. (2)); furthermore, it affects the apparatus handiness which is important for future use on scaffolding.
4. The measurement location, i.e. the microphone position x, controls the antiresonance frequencies as indicated in Eq. (3).
5. The pipe diameter Φ:
   (i) has to be large enough so as to supply an adequate amount of energy to the structure, in relation to the adsorption caused by the coupling between the acoustic device and the plaster;
   (ii) is limited by the resolution demanded in the detachment localisation;
   (iii) in order to comply with the assumption of plane waves, must be less than about $\frac{1}{5}$ the wavelength, $\Phi \leqslant (1/5)\lambda = (1/5)2\pi c/\omega$; hence it limits the utmost diagnosis frequency and consequently the chance of exciting the resonances of small detachments which have little compliance and mass;
   (iv) affects also the lowest test frequency, because it limits the diameter of the loudspeaker which the smaller it is, the less it is apt to emit in the low-frequency range.
6. The gasket used to ensure an airtight closure between the pipe extremity and the test surface is a crucial experimental element. Indeed, even a tiny fissure, allowing air leakage, can significantly bias the measures; all the same, a light contact force is advisable in order to prevent the gasket

from both spoiling the fresco and unduly damping the structural vibrations. To comply these demands, gaskets made of soft, compliant, closed cell foam rubber were properly designed.

Considering that the fresco structural dynamics are affected by the excitation frequency (item 1) and that the acoustic–structural interaction effects are evident around the antiresonances (item 2), in order to obtain various frequency intervals of analysis (items 3 and 4) different set-ups have been adopted. Frequency bands embodying either a resonance or antiresonance were analysed, but generally most significant information has been obtained considering the first antiresonance centred between the first two resonances.

The experimental data are analysed evaluating the acoustic FRFs, defined by the ratio of the acoustic pressure over the loudspeaker diaphragm velocity. The former quantity is gauged by a microphone properly positioned inside the pipe and the latter is evaluated by means of the current feeding the loudspeaker coil. The excitation is either a deterministic frequency sweep or a random signal, like a band limited white noise. The detachment is detected by comparing the indicator values stemming from the scan throughout the plaster surface. At each measure location, the indicator value is representative of the whole plaster area closing the duct and is attributed to the centre point. As a result, the indicator values are represented with the help of contour plots which are obtained by interpolating the actual measurements, to improve the intelligibility.

Although several configurations were adopted, only the results relative to two arrangements are reported. The main distinction between the two set-up configurations concerns the excitation frequency band which, affecting the vibrational behaviour of the specimens, characterises the detachment indicator. Hence, in order to analyse two contiguous frequency interval, two different set-ups has been adopted (Table 1). The two frequency intervals of analysis are able to produce

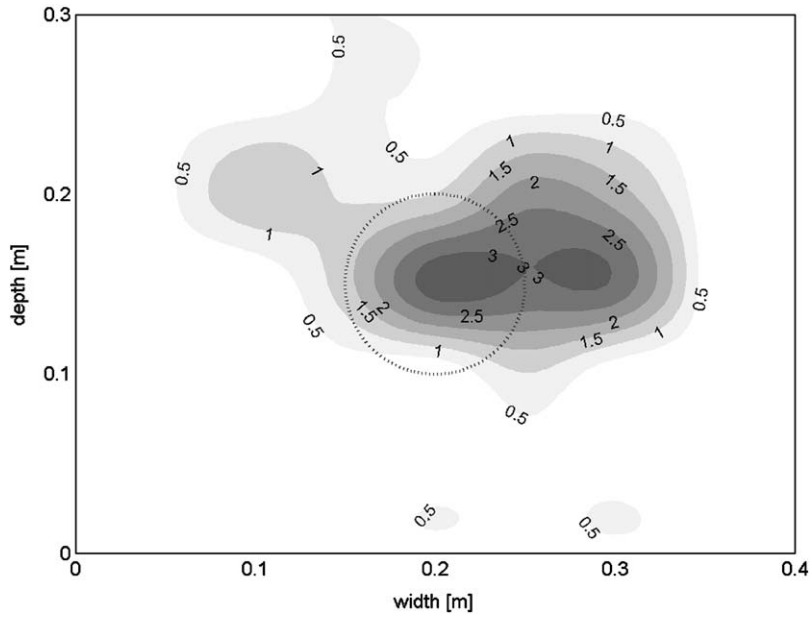

Fig. 9. Specimen 1: frequency range 400–620 Hz.

the two situations highlighted in Section 2.2, i.e. the case in which the structural resonances dominates the indicator value and the case in which the previous phenomenon is negligible and only the global energy flow contributes to the indicator. In both set-ups, the utmost frequency of

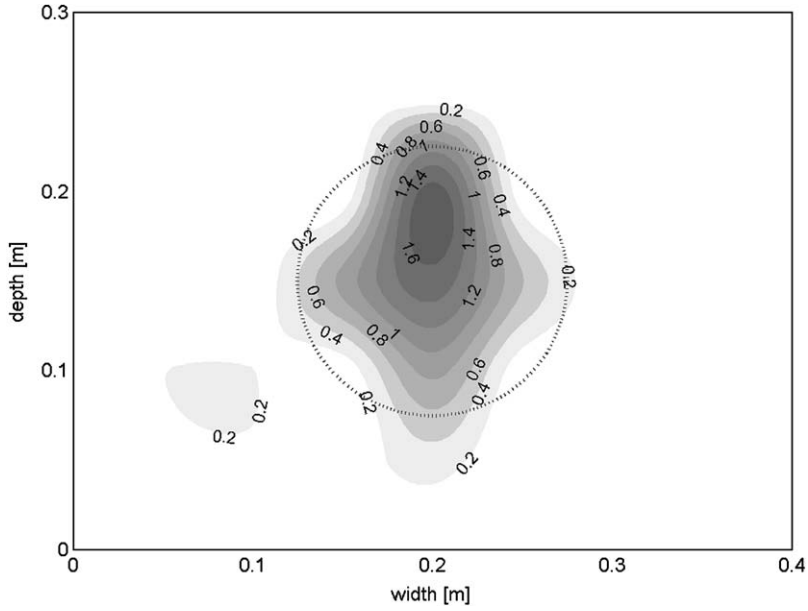

Fig. 10. Specimen 2: frequency range 400–620 Hz.

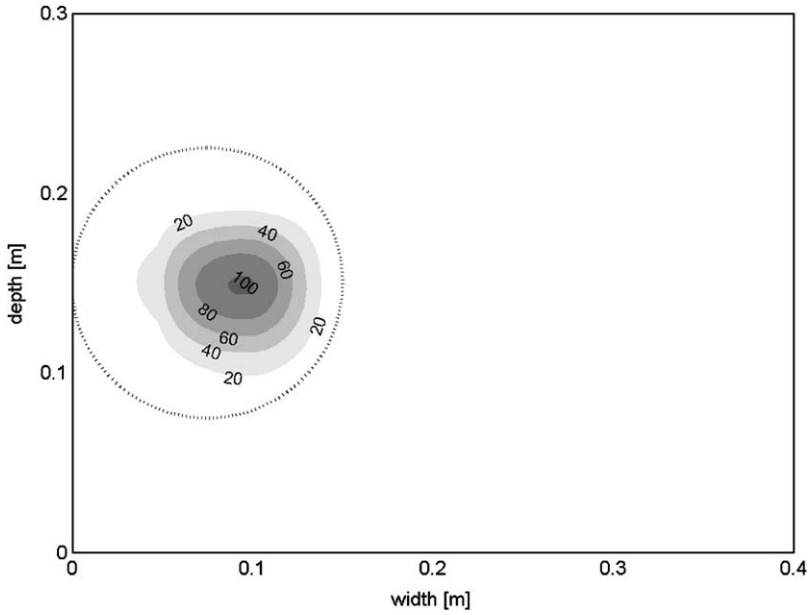

Fig. 11. Specimen 3: frequency range 400–620 Hz.

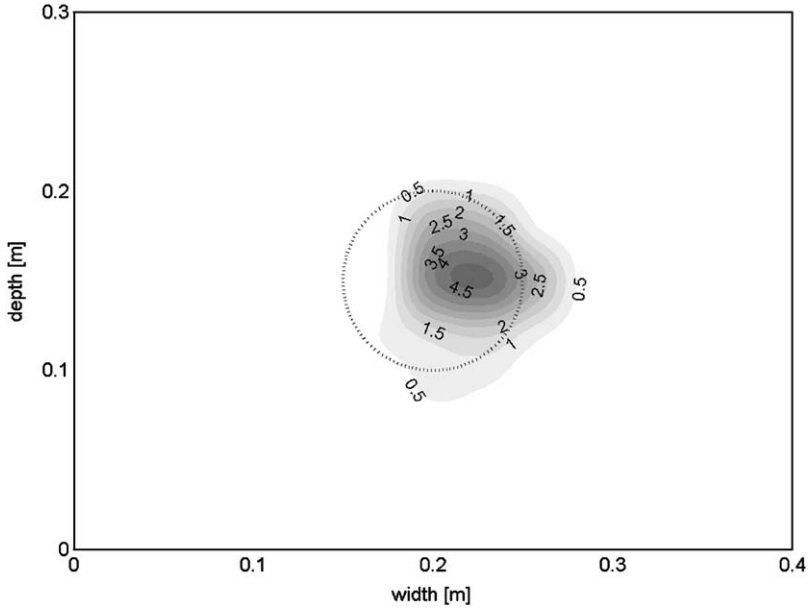

Fig. 12. Specimen 1: frequency range 620–920 Hz.

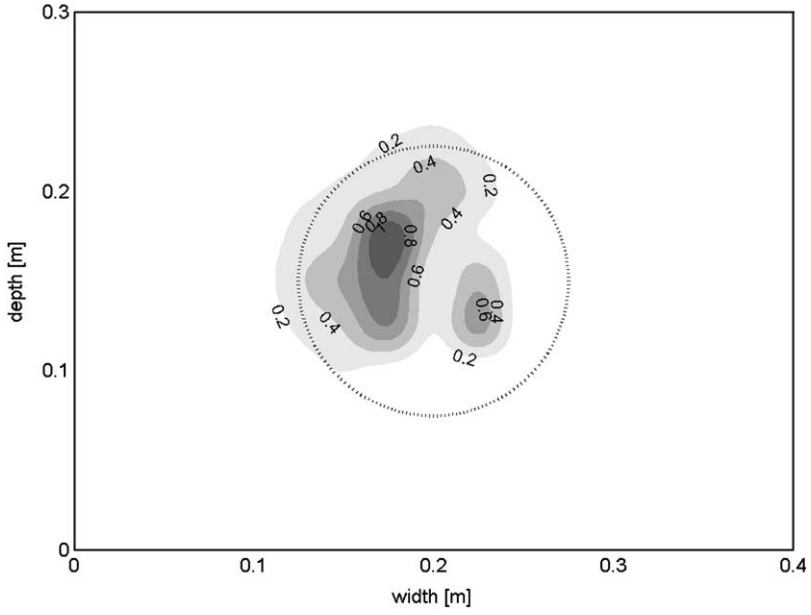

Fig. 13. Specimen 2: frequency range 620–920 Hz.

excitation is 941 Hz (item 5) and the frequency interval of diagnosis is centred around the first antiresonance which is approximately located in the middle of the first two resonances. Different loudspeakers were employed to supply adequate acoustical emission in the two frequency intervals.

3.2. Result examination

In this section some significant results are reported and interpreted. The description is restricted to the two set-ups in Table 1 and the three specimens in Fig. 8. In Figs. 9–14 the indicator values are represented through interpolated contour plots, together the trace of the appropriate detachment.

All the tests carried out with this experimental approach demonstrate that the proposed technique is effective, but manifests various degrees of sensitivity in the damage assessment. These and other features can be suitably illustrated commenting Figs. 9–14.

Taking into account the effect of structural resonances and of the energy flow, the results can be interpreted as follows. The results in Figs. 9, 12, 11 and 14, related to Specimens 1 and Specimen 3 excited in both bands, belong to the former situation. Indeed, the structural resonances control the detachment indicator and the energy flow has a much less effect. The reliability of the diagnosis is stated by the comparison between these contour plots and the detachment traces, despite the little discrepancies in Figs. 9 and 14 below considered. Fig. 13, related to Specimen 2 in the higher band of excitation, is an instance of the latter situation. Although in this case the detachment is clearly identified, in general the absence of structural resonances makes the indicator intensity to be small and this fact can lead to possible assessment uncertainties. Fig. 10,

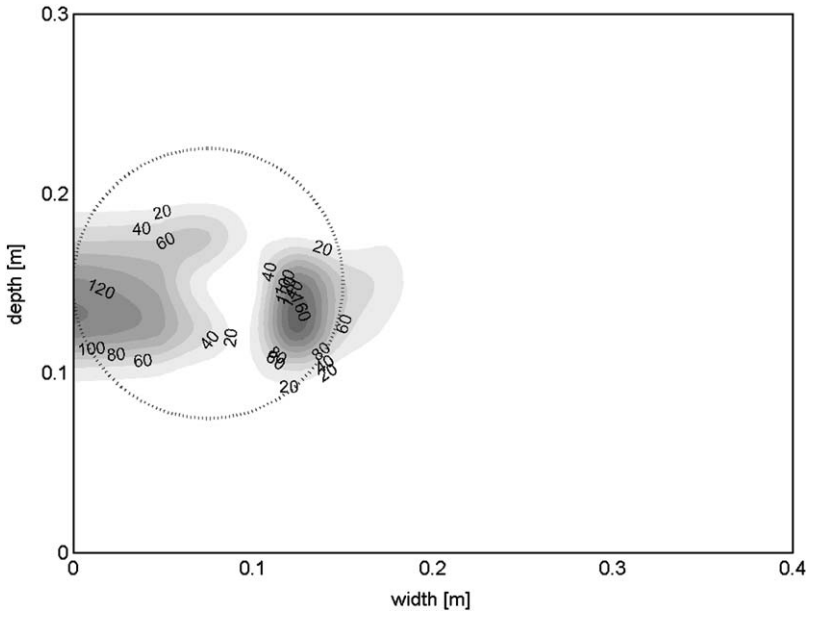

Fig. 14. Specimen 3: frequency range 620–920 Hz.

related to Specimen 2 excited in the lower frequency range, represents an intermediate situation, since both structural resonances and global energy flow contribute significantly to the detachment indicator.

Besides the preceding remarks, further considerations may be deduced from a survey of the results and considering that the specimens are structures which have parts with very different geometries joint together and therefore the detachment can be reckoned as an almost independent substructure.

- When the indicator is governed by the structural resonances (Figs. 9, 11, 12 and 14), it has higher levels and the damage assessment is more reliable than in the case in which the variation of the loss factor is the only symptom of the detachment (Fig. 13). Hence, very small detachments need high diagnosis frequency interval to be detected.
- In some cases, like Specimens 1 and 3, respectively, in the lower and higher frequency range (Figs. 9 and 14), although the indicator is mainly determined by the structural resonance contribution, irregular shapes are obtained. These situations are caused by the peculiar vibration distributions over the plaster surface. Specifically, the following situations can be recognized:
  (i) in the case of Fig. 9, as the detachment substructure is somewhat rigid with respect to the diagnosis frequency band, the excited structural resonance scantily involves in it; for this reason only low indicator increments are attained in the detachment region and interferences on the part of secondary phenomena cannot be avoided;
  (ii) in the case of Fig. 14, the excited structural mode has a nodal line which produces in correspondence of the detachment an antisymmetric shape: for some measurement locations the interaction between this mode and plane waves is negligible.
- Examining analogous situations, it has been noticed that the indicator shows greater values in the higher frequency band, i.e. using the shorter pipe. For the instances here considered this can be verified comparing
  (i) the case of Fig. 12 with the one of Fig. 9;
  (ii) the case of Fig. 14 with the one of Fig. 11.

4. Concluding remarks

In this work an experimental procedure for the diagnosis of fresco detachments is proposed. It is based on analysis of the plaster vibrational properties, evaluated by measuring the FRFs of an acoustic system coupled with the structure.

The test set-up required for the implementation of this method is quite simple, not expensive and, with straightforward automation, suitable for unskilled operator usage.

The results obtained with tests on mock-ups of frescoed structures are encouraging. Detachments are detected through an indicator, which is sensitive to the perturbation of the acoustic FRF phase around the antiresonances, produced by two separate phenomena: the interaction of structural resonances, which generates irregularities in the response, and the net flow of the acoustical energy towards the wall, which makes the loss factor increase. The indicator is particularly effective when structural resonances involving the detachment manifest their

presence: in such a case the detachment locations are correctly found out, regardless of the frequency band of analysis. In contrast, when the loss factor alteration is the unique sign of the acoustic–structural interaction, difficulties can arise. As a consequence, considering that the upper frequency of diagnosis is limited, detachments smaller than a certain threshold are difficult to detect; on the other hand, they are not relevant for fresco conservation. Furthermore, at the present stage, this method provides poor information about the detachment size and depth.

To circumvent these problems and broaden the scope of the technique, some improvements are recommended. A smarter indicator formulation can enhance the sensitivity to the acoustical energy flow, reducing the cited difficulties. In addition, the analysis could be performed over two or more intervals each one including an antiresonance, in order to expand the chance of exciting structural resonances. The closure system between the pipe and the fresco should be properly devised with the aim of minimizing the pressing force, not only to prevent the contact from damping the vibrations and thus hiding the detachment, but also to avoid any damage to the work of art. Other developments concern the possibility to automatically scan the fresco surface, following a definite grid and with a controlled contact force.

Acknowledgements

This research is supported by grants of MIUR (Italian Ministry for Education, University and Research).

References

[1] G. Schirripa Spagnolo, G. Guattari, E. Grinzato, P.G. Bison, D. Paoletti, D. Ambrosini, Frescoes diagnostics by electro-optic holography and infrared thermography, in: *Sixth World Conference on NDT and Microanalysis in Diagnostics and Conservation of Cultural and Environmental Heritage (AIPnD)*, Rome, Italy, 1999.

[2] E. Grinzato, G.P. Bison, S. Marinetti, V. Vavilov, Thermal NDE enhanced by 3D numerical modeling applied to works of art, in: *15th World Conference on Non-Destructive Testing*, Rome, Italy, 2000.

[3] P. Desiderio, M. Prencipe, FRP Plating inspection on static consolidation of buildings by infrared video thermography and low frequency (microseismic) ultrasound, in: *Proceedings of the 15th World Conference on Non-Destructive Testing*, Rome, Italy, 2000.

[4] M.A. Knight, G. Cascante, M.C. Lopez, Laboratory investigation into the assessment of concrete pipes state of deterioration using ultrasonic testing techniques, in: *International Conference on Underground Infrastructure Research, UIR 2001*, Kitchener, Ontario, 2001.

[5] M. Krause, C. Maierhofer, H. Wiggenhauser, O. Bärmann, K. Langenberg, R. Frielinghaus, J. Neisecke, F. Wollbold, M. Schickert, Comparison of pulse-echo-methods for testing concrete, *The e-Journal of Non-destructive Testing* 1 (10) (1996).

[6] H. Wenzel, *Structural Assessment of the Cultural Heritage*, Publication of VCE Consult ZT (GmbH), Vienna, Austria, 2002.

[7] A. Bonarrigo, G. Cucco, Evaluation for study and conservation of works of art, investigation of the conservation state of wall mosaics through analysis of dynamic signals, in: *Second International Conference on Non-Destructive Testing, Microanalytical Methods and Environment*, Perugia, Italy, 1988.

[8] W. D'Ambrogio, A. Mannaioli, D. Del Vescovo, Use of FRF measurements as a non-destructive tool to detect detachments of frescoes, in: *XII International Modal Analysis Conference*, Honolulu, Hawaii, 1994, pp. 1083–1088.

[9] P. Castellini, N. Paone, E.P. Tomasini, The laser Doppler vibrometer as an instruments for nonintrusive diagnostic of work of art: application to fresco paintings, *Optics and Lasers in Engineering* 25 (1996) 227–246.
[10] P. Calicchia, G.B. Cannelli, Revealing surface anomalies in structures by in situ measurement of acoustic energy absorption, *Applied Acoustic* 63 (2002) 43–59.
[11] D. Del Vescovo, A. Fregolent, An acoustic non invasive technique for the diagnosis of plaster detachment in Frescos, in: *XVII International Modal Analysis Conference*, Orlando, Florida, 1999, pp. 1405–1411.
[12] L.L. Beranek, *Acoustics*, McGraw-Hill, New York, 1954.